2017

Resident macrophages of pancreatic islets have a seminal role in the initiation of autoimmune diabetes of NOD mice

Javier A. Carrero
Washington University School of Medicine in St. Louis

Derrick P. McCarthy
Washington University School of Medicine in St. Louis

Stephen T. Ferris
Washington University School of Medicine in St. Louis

Xiaoxiao Wan
Washington University School of Medicine in St. Louis

Hao Hu
Washington University School of Medicine in St. Louis

See next page for additional authors

Resident macrophages of pancreatic islets have a seminal role in the initiation of autoimmune diabetes of NOD mice

Javier A. Carrero[a,1], Derrick P. McCarthy[a,1], Stephen T. Ferris[a,1], Xiaoxiao Wan[a,1], Hao Hu[a], Bernd H. Zinselmeyer[a], Anthony N. Vomund[a], and Emil R. Unanue[a,2]

[a]Department of Pathology and Immunology, Washington University School of Medicine, St. Louis, MO 63110

Contributed by Emil R. Unanue, October 21, 2017 (sent for review August 1, 2017; reviewed by Pere Santamaria and David V. Serreze)

Treatment of C57BL/6 or NOD mice with a monoclonal antibody to the CSF-1 receptor resulted in depletion of the resident macrophages of pancreatic islets of Langerhans that lasted for several weeks. Depletion of macrophages in C57BL/6 mice did not affect multiple parameters of islet function, including glucose response, insulin content, and transcriptional profile. In NOD mice depleted of islet-resident macrophages starting at 3 wk of age, several changes occurred: (*i*) the early entrance of CD4 T cells and dendritic cells into pancreatic islets was reduced, (*ii*) presentation of insulin epitopes by dispersed islet cells to T cells was impaired, and (*iii*) the development of autoimmune diabetes was significantly reduced. Treatment of NOD mice starting at 10 wk of age, when the autoimmune process has progressed, also significantly reduced the incidence of diabetes. Despite the absence of diabetes, NOD mice treated with anti–CSF-1 receptor starting at 3 or 10 wk of age still contained variably elevated leukocytic infiltrates in their islets when examined at 20–40 wk of age. Diabetes occurred in the anti–CSF-1 receptor protected mice after treatment with a blocking antibody directed against PD-1. We conclude that treatment of NOD mice with an antibody against CSF-1 receptor reduced diabetes incidence and led to the development of a regulatory pathway that controlled autoimmune progression.

macrophage | islets of Langerhans | type 1 diabetes | nonobese diabetic mouse | regulation

Tissue-resident macrophages constitute a heterogeneous and multifunctional cell type that populates virtually every tissue (reviewed in refs. 1 and 2). In addition to their primary role as sentinels for invading pathogens and as initiators of inflammation, macrophages have important homeostatic roles in many tissue-specific processes such as development, metabolism, and tissue remodeling, providing trophic factors within the tissue microenvironment. Their homeostatic role is evidenced by the deleterious phenotype that arises when macrophage development is genetically constrained. The osteopetrotic mouse (*op*/*op*) harbors a severe paucity of macrophages due to a null mutation in the gene encoding the macrophage differentiation and survival factor, colony stimulating factor-1 (CSF-1) (3). These mice present with a number of developmental defects. Notably, the islets of Langerhans, which normally contain a population of CSF-1–dependent macrophages, are atrophic in the *op*/*op* mouse, suggesting an integral role for macrophages during the development of the endocrine pancreas (4, 5).

The pancreatic islets of all species contain a small number of myeloid cells represented by macrophages. These macrophages were first identified by immunohistochemical analysis using macrophage-specific markers. Although initially thought to be "passenger leukocytes," subsequent studies using lineage tracing approaches identified them as resident cells (5). These self-replicate and are replaced minimally, if at all, by blood monocytes. Islet macrophages are highly activated with a complex gene transcriptome reflecting their interactions with beta cells and with blood components (6). They express high levels of class II histocompatibility molecules (MHC-II) and a number of cytokines and chemokines including TNF-α and IL-1β (5, 6). The islet macrophages are always next to blood vessels, in close contact with beta cells, capture insulin-containing granules, and present insulin peptides to autoreactive CD4 T cells (7). Moreover, macrophages extend filopodia into the vessel lumen and can respond to blood stimuli (6, 8).

Our laboratory focuses on the early events that initiate autoimmune diabetes as exemplified in the NOD mouse strain. Understanding the initiation of autoimmune diabetes is of considerable clinical interest. Along those lines, identifying the key cellular and molecular events that transition the immune-privileged islet to an immunologically reactive environment is paramount as it pertains to diabetes initiation. By 3 wk of age, islets show significant cellular and molecular changes compared with nondiabetic strains: an early entrance of $CD4^+$ T cells reactive to insulin in contact with the macrophages, a heightened gene signature of activation in the macrophages, and the appearance of the $XCR1^+$ subset of dendritic cells (DCs) (9, 10). The deficit of $XCR1^+$ DCs in the NOD *Batf3*$^{-/-}$ mice translates into a profound reduction in the autoimmune process (10).

Here, we examine the role of the resident macrophages in diabetogenesis. The islet macrophage expresses both inhibitory and stimulatory ligands and receptors, as well as chemokines and

Significance

Our studies indicate that the resident macrophages of the pancreatic islets of Langerhans have a seminal role in the initiation and progression of autoimmune diabetes in NOD mice. In this study, islet macrophages were depleted by administration of a monoclonal antibody to the CSF-1 receptor. Macrophage depletion, either at the start of the autoimmune process or when diabetogenesis is active, leads to a significant reduction in diabetes incidence. Depletion of the islet macrophages reduces the entrance of T cells into islets and results in the absence of antigen presentation. Concordantly, a regulatory pathway develops that controls diabetes progression. We conclude that treatments that target the islet macrophages may have important clinical relevance for the control of autoimmune type 1 diabetes.

Author contributions: J.A.C. and E.R.U. designed research; J.A.C., D.P.M., S.T.F., X.W., H.H., B.H.Z., and A.N.V. performed research; J.A.C., D.P.M., S.T.F., X.W., H.H., B.H.Z., A.N.V., and E.R.U. analyzed data; and J.A.C. and E.R.U. wrote the paper.

Reviewers: P.S., University of Calgary; and D.V.S., The Jackson Laboratory.

The authors declare no conflict of interest.

[1]J.A.C., D.P.M., S.T.F., and X.W. contributed equally to this work.

[2]To whom correspondence should be addressed. Email: unanue@wustl.edu.

This article contains supporting information online at www.pnas.org/lookup/suppl/doi:10.1073/pnas.1713543114/-/DCSupplemental.

chemokine receptors (6). They are the sole hematopoietic cell within the islets before 3 wk of age and are able to present unconventional insulin epitopes to autoreactive T cells (6). Altogether, this posits the intraislet macrophage as a key regulator of lymphocyte entry into the islet. We have eliminated them using a monoclonal antibody to the CSF-1 receptor (CSF-1R), AFS98 (11). This monoclonal antibody, and the M279 antibody against CSF-1R, when administered in vivo resulted in the loss of macrophages from many tissues (12–14). The extent of depletion depended on the amount and frequency of administration (12). Although treatment with AFS98 resulted in the loss of resident macrophages, blood monocyte counts and inflammatory responses were not affected (13). We present evidence that the anti–CSF-1R antibody AFS98 depleted the islet resident macrophages in two strains of mice: the normal C57BL/6 (B6) and the diabetogenic NOD. The depletion of macrophages did not affect the metabolism or islet transcriptome of the mouse. However, diabetes progression was severely blunted.

Results

Evaluation of C57BL/6 Mice. First, we evaluated the nondiabetic B6 strain, following treatment with the monoclonal antibody against CSF-1R. Injecting B6 mice with 0.25, 0.50, and 2.0 mg of AFS98 led to a dose-dependent elimination of the intraislet macrophages (Fig. 1*A*). This reduction was observed as early as 7 d after treatment and was equally evident at day 14. The depletion was long lived. A 2.0-mg dose of AFS98 resulted in elimination of the islet macrophage lasting for at least 6 wk (Fig.

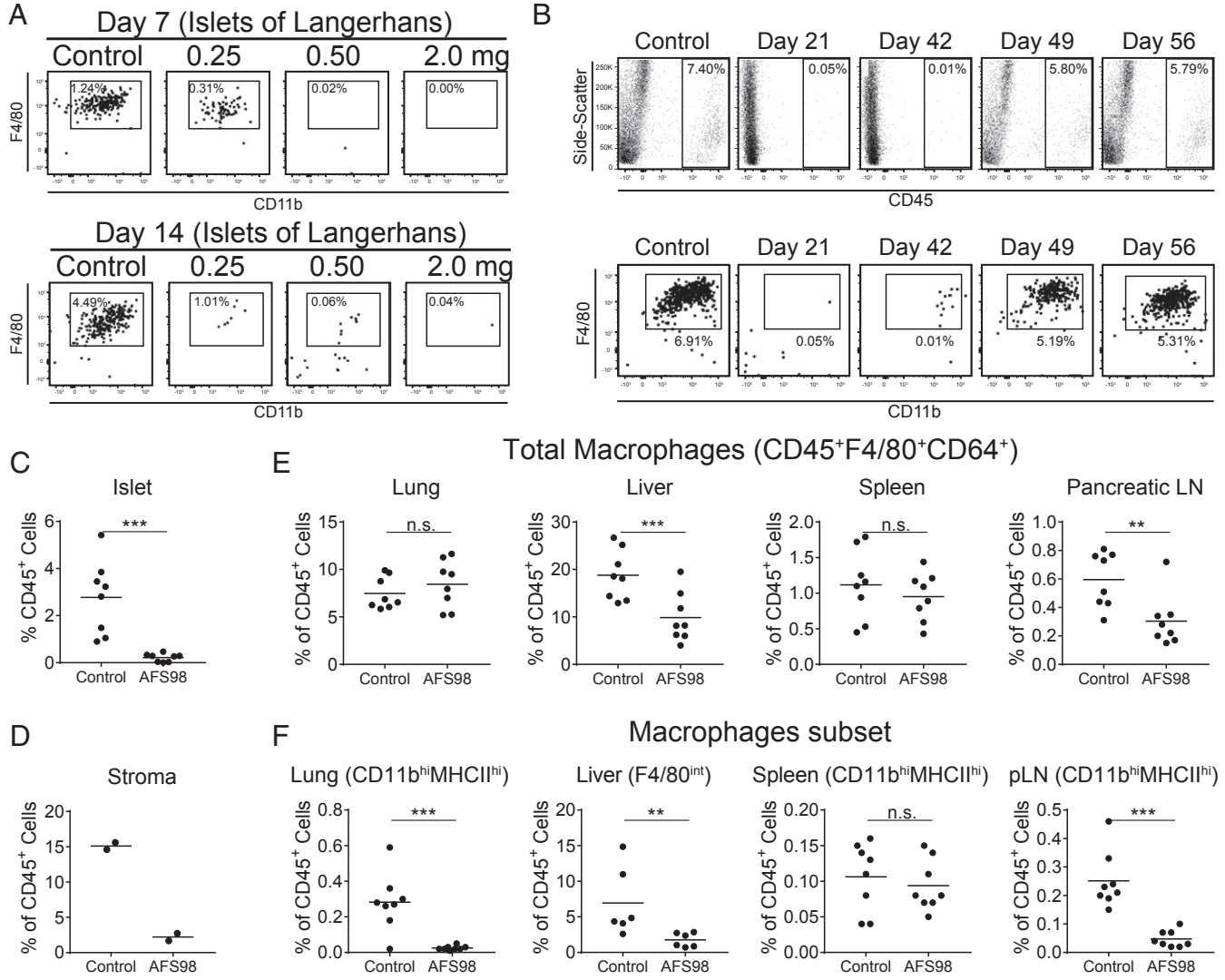

Fig. 1. Treatment of C57BL/6 mice with AFS98 antibody depleted their macrophages. (*A*) Female B6 mice aged 6–8 wk were administered 0.25, 0.50, or 2.0 mg of AFS98 antibody i.p. Islets were examined 7 and 14 d after injection for the presence of macrophages. Box indicates $CD45^+CD11c^+MHCII^+F4/80^+CD11b^+$ cells as a percent of total islet cellularity. (*B*) Female B6 mice aged 6–8 wk were treated with 2.0 mg of AFS98, and their islets were examined at the time points indicated for the presence of macrophages. *Top* show the $CD45^+$ cells, and *Bottom* show the $CD45^+CD11c^+MHCII^+$ $F4/80^+CD11b^+$ cells as a percent of total islet cellularity. (*C*) Graph of the $CD45^+$ cells found in mice 1–2 wk after treatment with 2.0 mg of AFS98. (*D*) Graph of $CD45^+F4/80^+CD64^+$ islet stromal macrophage populations as a percent of $CD45^+$ cells in control and AFS98-treated mice 2 wk after treatment. (*E*) Mice were treated for 1–2 wk with AFS98 antibody, and the percent of total macrophages in lung, liver, spleen, and pancreatic lymph nodes were determined. (*F*) Macrophages were examined as in *E* except plots show the percent of the indicated subpopulation of macrophages. For all graphs, controls were untreated age-matched mice. Flow cytometry plots in *A* and *B* are representative of individual islet, lung, liver, spleen, and lymph nodes, from two to three experiments with two to four mice per treatment group. Scatter plots in *E* and *F* were calculated from three independent experiments with two to three mice per group. *P* values were calculated using Mann–Whitney *U* test with the following style: not significant (n.s., >0.1234), $*P = 0.0332$, $**P = 0.0021$, $***P = 0.0002$, $****P < 0.0001$.

1*B*). Macrophages started to return to the islets by 6 wk and were at normal levels by 7 wk after antibody treatment. The depletion of macrophages in the islets was consistent over multiple experiments (Fig. 1*C*). The macrophages of the stroma were also affected by the AFS98 treatment. The macrophage reduction was almost complete resulting in an ∼85% reduction compared with control-treated mice (Fig. 1*D* and Fig. S1).

In addition to islets, several other tissues were examined. In most, a set of the resident macrophages was also affected 7–14 d after antibody administration. We analyzed total macrophages by expression of F4/80 and CD64 and calculated their reduction as shown in Fig. 1*E*. However, it was evident that the sensitivity to AFS98 treatment was variable (Fig. 1*F*). In the lung, alveolar macrophages were not affected, yet the $CD11b^{+}$ interstitial macrophages were depleted (15) (Fig. 1 *E* and *F*). In the liver, there are two macrophage populations defined by expression of F4/80. The $F4/80^{hi}$ Kupffer cells were reduced by about 50% (Fig. 1 *E* and *F*). The $F4/80^{int}$ monocyte-derived macrophages were almost completely depleted by AFS98 treatment. This last finding suggest that these macrophages most likely represent the recently identified liver capsular macrophages (16). The spleen macrophages were not affected (Fig. 1 *E* and *F*). However, in the pancreatic lymph node, a set of macrophages characterized by CD11b (similar in surface marker expression to the lung interstitial macrophages) were >80% reduced. Thus, not all tissue macrophages are as sensitive to anti–CSF-1R as the ones in the islets.

In summary, treatment with AFS98 led to variable effects on the macrophages residing in various tissues, while in islets, the effects were pronounced and prolonged. We also evaluated whether AFS98 treatment could affect the number of T and B cells and their differentiation in thymus and bone marrow. We found no impairment in their numbers and differentiation patterns in thymus or bone marrow (Fig. S2).

As seen in the *op*/*op* mouse, the absence of macrophages from birth can lead to systemic disruption of mouse homeostasis. Therefore, we evaluated two basic parameters of islet function after macrophage depletion: glucose tolerance and beta-cell insulin content. The glucose tolerance test measures the ability of the beta cell to sensor and respond to glucose, release insulin, and return the mouse to euglycemia. Following treatment of the B6 mice with the AFS98 antibody, neither glucose tolerance nor insulin content was affected (Fig. 2 *A* and *B*). Glucose tolerance was unimpaired even after 6 wk of macrophage depletion in the islets (Fig. 2*A*). Measured pancreatic insulin content was stable at 3 wk after depletion (Fig. 2*B*).

A more global and unbiased measure of islet health is to evaluate the whole transcriptome. B6 mice were treated with 2.0 mg of AFS98 or control $IgG2_a$ at 3 wk of age, and whole islets were isolated at 6 wk of age. Comparison of AFS98 versus $IgG2_a$-treated mice revealed 16 differentially expressed transcripts at a twofold change and 99% confidence interval in whole islets (Fig. 2*C*). These 16 changes were in transcripts known to be encoded strictly by the macrophage. These included transcripts previously reported to be up-regulated during diabetes progression (9). Therefore, the majority of the islet transcriptome was not significantly affected by macrophage depletion, and the only change was the loss of the islet macrophage. In conclusion, homeostasis of islet function was not affected in a detectable manner when macrophages were depleted several weeks after birth.

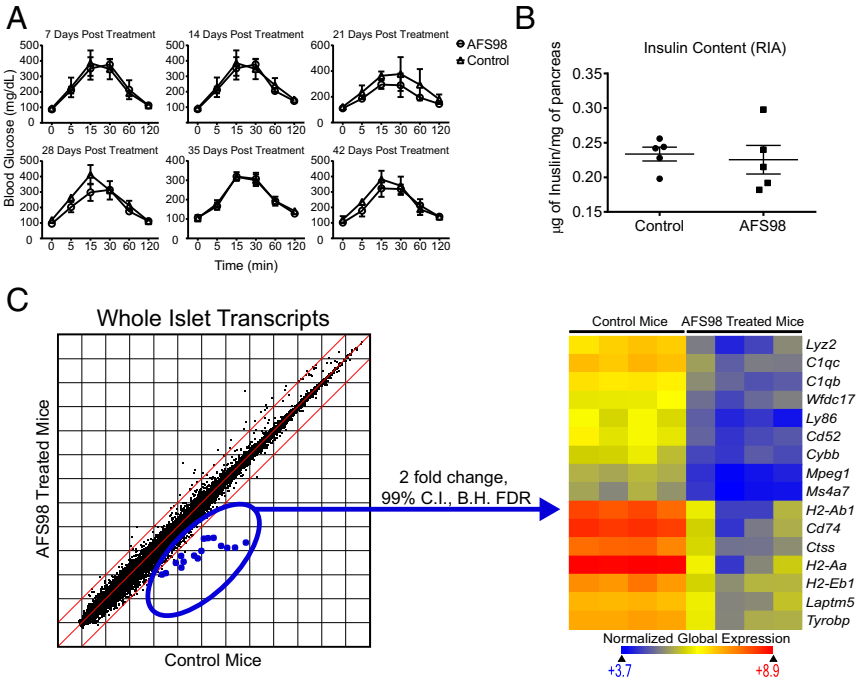

Fig. 2. Islet function after depletion of macrophages by AFS98. (*A*) B6 mice were given 2.0 mg of AFS98 i.p. at 6–8 wk of age. Glucose tolerance assays were then performed on AFS98-treated and untreated mice. After the indicated number of days, the mice were fasted for 12 h and then injected with 2.0 g/kg glucose i.p. Blood glucose (mg/dL) was measured at the indicated time points. Results are pooled from two independent experiments (n = 2–3 mice per group). (*B*) Nine-week-old B6 females were left untreated or administered 2.0 mg of AFS98 i.p. Four days later, the mice were placed on a 20% sucrose diet for an additional 7 d, then returned to a normal diet for 2 d. The mice were then killed, and the insulin content of their islets was measured (n = 5 mice per group). (*C*) Three-week-old C57BL/6 mice were left untreated or administered 2.0 mg of AFS98 i.p. At 6 wk of age, their islets were isolated, total RNA was extracted, and transcripts were analyzed by microarray. Scatter plot shows the $\log_2$ mean expression values for four control and experimental mice. The dots highlighted in blue represent genes differentially expressed between treated and control mice at 99% confidence using moderated t test with Benjamini–Hochberg false discovery rate analysis. The selected genes are plotted in the heat map using Euclidean distance and normalized global expression as indicated.

Evaluation of NOD Mice.

Islets. Similar to the results observed in B6 mice, Fig. 3*A* shows that treatment with 0.5 or 2.0 mg of AFS98 depleted the islet macrophages in 4- to 5-wk-old NOD mice. Comparable results were obtained following treatment of NOD.*Rag1*$^{-/-}$ mice with the AFS98 antibody (Fig. S3). An analysis of NOD mice at 3–4 wk of age showed that the initial islet infiltrating T cells were all CD4$^+$ and mostly in contact with the intraislet macrophage (9). The islet macrophages express CD11b, CD11c, and MHC-II highly on their surface. At this 3–4 wk of age period, there are very few XCR1$^+$ DCs in islets (10).

We confirmed the colocalization of CD4 T cells with intraislet macrophages by examining islets using two-photon microscopy. NOD mouse islets were examined at 3–4 wk of age, the earliest age where one can identify the initial infiltrating T cells. Indeed, 27% of NOD islets had CD4 T cells, 70% of which were in contact with the F4/80$^+$ macrophages, confirming our initial studies. In the mice that were injected with 0.5 mg of anti–CSF-1R at 2 wk of age, the islets did not harbor any myeloid cells at 4 wk of age. In these mice, only 3% of islets had a detectable CD4 T cell.

Next, we examined insulin peptide presentation by isolating the islets, dispersing the cells, and culturing them with insulin-reactive CD4 T cell hybridomas. Depletion of islet macrophages resulted in marked reduction of presentation to two different CD4 T cell hybridomas recognizing different MHC-II epitopes of insulin (17). The addition of the cognate peptides reflects the availability of MHC-II$^+$ presenting cells. As noted in Fig. 3*B*, this addition did not lead to presentation in the islets of the treated mice, reflecting the paucity of presenting cells and the inability of any other islet cell to express MHC-II or present peptide. The same findings were reproduced in B6.g7 mice (Fig. S4).

Lymph node responses. While the islets from the macrophage-depleted mice were impaired in antigen presentation, this was not the case in the peripheral lymph nodes. This was determined using two approaches: carboxyfluorescein succinimidyl ester (CFSE) dilution of transferred T cells and recall response by ELISpot. For CFSE dilution experiments, we transferred CD4 (BDC2.5) or CD8 (NY8.3) T cell clones into control or AFS98-treated NOD. BDC2.5 responds to a chromogranin peptide in the context of I-A^{g7} (18), while the NY8.3 T cell divides in response to a peptide derived from IGRP, the islet-specific glucose-6-phosphatase–dependent catalytic subunit-related protein, in the context of H-2Kd (19, 20). Fig. 4 *A* and *B* shows that both T cell clones proliferated in the draining pancreatic lymph node, but not in the distant inguinal lymph node. Next, to determine if depletion of the islet macrophage affected the trafficking of diabetogenic cells to the islets, we examine the entrance of TCR transgenic T cells into them. Both BDC2.5 and NY8.3 T cells entered islets of control mice but neither entered the islets from AFS98-treated mice (Fig. 4*C*). While the T cells entered and reacted to antigen presented in the pancreatic lymph node, this was not the case in the islets.

In the second approach, AFS-treated mice were immunized with various autoreactive peptides in the footpads and the T cell response was tested a week later; there was no impairment of the response (Fig. 5). Immunization with the insulin B:9–23 peptide elicited an IL-2 and IFN-γ response to the peptide but not to the insulin protein, as reported before (17). Immunization with peptides from IGRP known to elicit CD4 or CD8 T cell responses was also unaffected by AFS98 treatment. The CD4 or CD8 T cell responses to the foreign protein hen egg lysozyme (HEL) were also unaffected.

In brief, examination by flow cytometry, direct microscopy of islets, antigen presentation assays, and T cell migration assays shows that the lack of macrophages translates into an absence of early CD4 T cell infiltration and antigen presentation capability of the islets. In contrast, the lymph nodes in the AFS-treated mice were active in antigen presentation.

Diabetes. Female NOD mice were followed for diabetes after treatment with AFS98 or control rat IgG2$_a$ antibody. In two experiments, mice were treated at 2–3 wk of age, a time when the diabetogenic process is starting in limited islets. The treatment was continued for several weeks using two different concentrations of antibody. In a third experiment, NOD mice were treated starting at 10 wk of age, a time when the diabetogenic process is active and most islets are already infiltrated by both CD4 and CD8 T cells. Both treatments led to a marked reduction in diabetes incidence when the mice were followed for 40 wk. The pooled results are shown in Fig. 6*A*. Fig. 6*C* shows the results of the individual experiments. Combining the three experiments, 4 of 40 AFS98-treated mice and 24 of 39 of the control mice became diabetic.

At the end of the 40–42 wk of observation, two manipulations were performed on the AFS98-treated mice. First, the mice were administered an anti–PD-1 monoclonal antibody and this led to

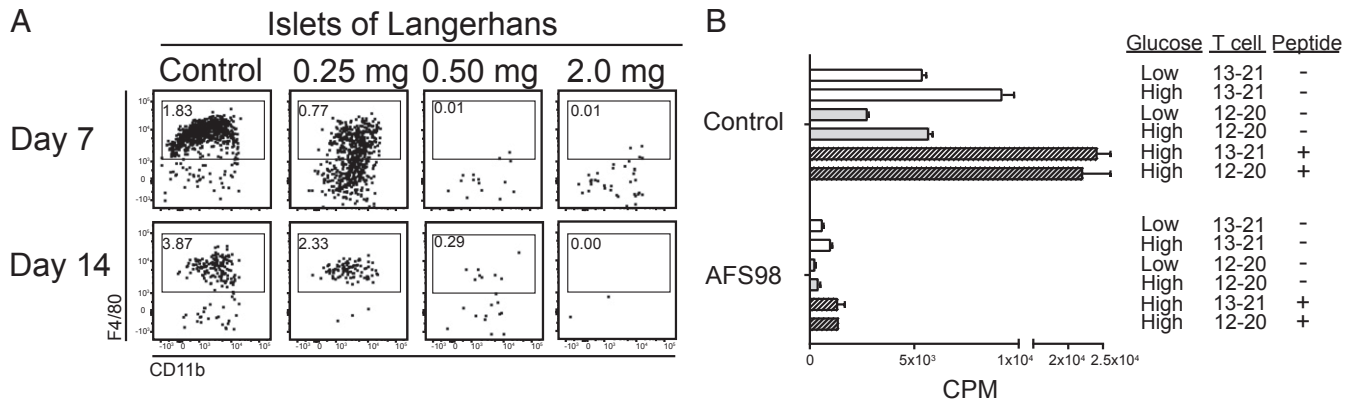

Fig. 3. Effect of AFS98 treatment on NOD mice. (*A*) Male NOD mice at 4–5 wk of age were administered 0.25, 0.50, or 2.0 mg of AFS98 i.p., and their islets were examined by flow cytometry. Plots show the CD45$^+$CD11c$^+$MHCII$^+$ gate at either 7 or 14 d after treatment. Results are representative of two experiments performed in duplicate. Values in the box represent the percent of cells as a function of total islet cellularity. (*B*) Two-week-old male NOD mice were left untreated (Control) or injected i.p. with 0.5 mg of AFS98 at 2 wk of age and 2.0 mg of AFS98 at 4 wk of age (AFS98). At 6 wk of age, the islets were harvested, dispersed, and tested for their MHCII-peptide presentation to two T cell hybridomas that recognize insulin. High (25.0 mM) or low (5.0 mM) glucose and two different insulin peptides (Ins B:12–20 and Ins B:13–21) were evaluated. Bars represent the mean ± SD of ^{3}H incorporation by the IL-2–dependent cell line CTLL-2.

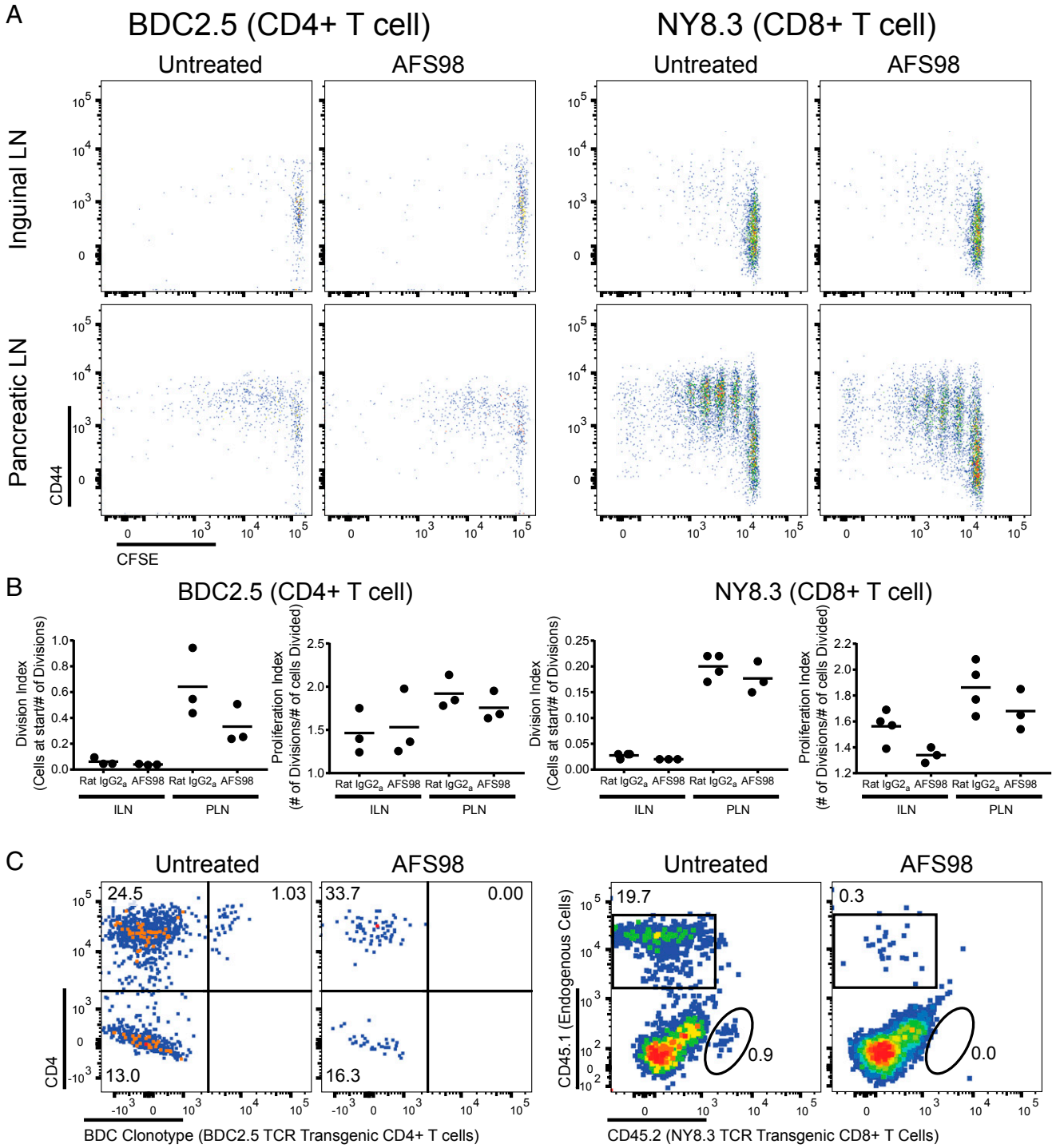

Fig. 4. AFS98 treatment does not affect T cell division in lymph nodes but prevents T cell entry into islets of Langerhans. NOD mice were injected with AFS98 antibody at a dose of 0.5 mg at 2 wk of age and 2.0 mg at 4 wk of age. Two TCR transgenic T cells, the $CD4^+$ BDC2.5 and the $CD8^+$ NY8.3, were isolated from lymph nodes and spleens of their respective mice. T cells were then labeled with CFSE and transferred into 6-wk-old NOD mice that had either been left untreated or treated with AFS98. (*A* and *B*) Seven days after T cell transfer, the pancreatic and inguinal lymph nodes were isolated and analyzed by flow cytometry. (*A*) Dilution of CFSE in either inguinal (*Upper*) or pancreatic (*Lower*) lymph nodes for an individual mouse per treatment is shown. Cells were gated on forward and side-scatter, CD45, CD3, and either CD4 (BDC2.5) or CD8 (NY.8.3). (*B*) Summary of division index and proliferation index for individual mice examined as in *A*. Results show three or four individual mice per group. (*C*) Ten days after TCR transgenic T cell transfer, islets of Langerhans were isolated and examined for entry of either the BDC2.5 or NY8.3 T cells by flow cytometry. The *Left* two images are gated on forward and side-scatter, CD45, and CD3. The *Right* images are gated on forward and side-scatter. BDC T cells were identified using a clonotypic antibody to its T cell receptor. NY8.3 T cells were identified by a CD45.2 congenic label. Numbers indicate the percent of cells in each selection as a function of $CD45^+$ cells. T cell islet entry results are representative of two to three independent experiments with two to four individual mice per group.

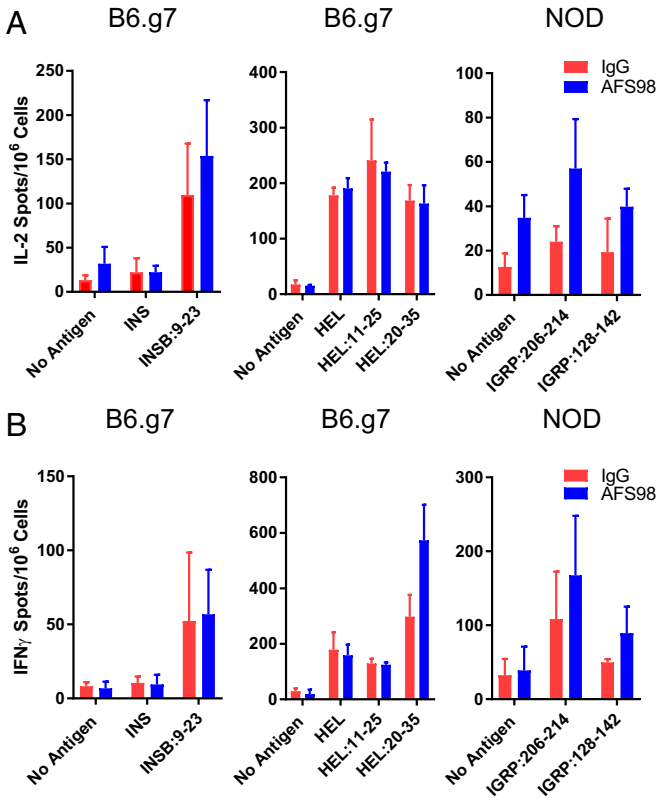

Fig. 5. Lymph node priming is not reduced by AFS98 treatment. B6.g7 or NOD mice were treated with 2 mg of AFS98 antibody for 1 wk and then injected with 10 nmols INS:9–23, HEL, or IGRP peptides in complete Freund's adjuvant. The draining popliteal lymph nodes were isolated and tested by ELISPOT for IL-2 (*A*) and IFN-γ (*B*) production. Recall antigens for the ELISPOT are shown in the figure and include the following: insulin protein (INS) and INS:9–23, HEL protein and peptides that elicit CD4 (11–25) and CD8 (20–35) responses, and the IGRP peptides that elicit CD4 (128–142) and CD8 (206–214) responses. Results are taken from two individual mice tested in duplicate or triplicate.

the rapid development of diabetes in 7 of 7 of the mice evaluated (Fig. 6*C*). Others have found a profound regulatory effect of the PD-1/PD-L1 pathways in regular diabetogenesis, and at least this pathway is operational following AFS98 treatment (21–23). Anatomically, insulin-reactive T cells express PD-1, while in islets the beta cells, vascular endothelium, macrophages, and inflammatory DCs express high levels of PD-L1 (21, 24, 25).

Second, splenocytes from the AFS98-treated mice were transferred into NOD.*Rag1*$^{-/-}$ mice. NOD splenocytes transfer disease to normally nondiabetic NOD.*Rag1*$^{-/-}$ mice and is used as a measure of the diabetogenic potential of the T cells in the NOD mouse following genetic or pharmaceutical manipulations. The mice first treated with AFS98 at the 2- to 3-wk period transferred diabetes poorly; only 1 of 14 became diabetic 20 wk after transfer (Fig. 6 *B* and *C*). In contrast, splenocytes from 10-wk, AFS98-treated NOD mice transferred diabetes to 8 of 8 recipients.

We also examined the islets for their leukocyte content at various time points after their treatment with AFS98. Fig. 7 shows results from mice treated at 2–3 wk of age. AFS98 treatment resulted in a reduction of total leukocytes (CD45$^+$) from ∼10% in controls to ∼1% in the treated mice by 8 wk after treatment (Fig. 7*A*). There was also a reduction of F4/80$^+$ macrophages from ∼4% of total islet cellularity to undetectable levels. Over time, the control NOD mice showed progressive increase in the CD45$^+$ cells (Fig. 7*B*). After the end of the observation period—at 44 wk—a number of the islets from AFS-treated mice were infiltrated. We observed two phenotypes: 4 of 8 mice contained ∼20–25% CD45$^+$ cells in the islets, and 4 of 8 mice contained 2–5% CD45$^+$ cells in the islets (Fig. 7 *C* and *D*). (The IgG-treated control NOD mice contained ∼60–70% CD45$^+$ cells in islets.) Corroborating the flow cytometry ∼50% of the pancreata examined had a degree of peri-insulitis (Fig. 7*E*). However, the other 50% of pancreata examined showed little to no insulitis (Fig. 7*F*). Therefore, macrophage depletion is protective in NOD mice long term, despite the infiltration or expansion of leukocytes in ∼50% of the mice.

In mice treated with AFS98 starting at 10 wk of age, there also was a reduction in the number of leukocytes in islets at 22 wk of age. However, by 40 wk of age, all of the mice had comparable infiltrates to a 22-wk-old NOD mouse (Fig. 8). Thus, late macrophage depletion does not stop the infiltration of islets, despite preventing the development of hyperglycemia.

These results suggest that macrophage depletion can act before and after the diabetogenic T cell pool in the NOD has fully developed. Early AFS98 treatment blocks diabetes by eliminating a key antigen-presenting cell in islets, preventing early entry of activated T cells, and limiting the expansion of the diabetogenic T cells. In contrast, in late-treated NOD mice, there are active diabetogenic T cells but disease is controlled by the development of a regulatory condition through at least one mechanism, PD-1/PD-L1 interaction. In both situations, we find islet infiltration with preservation of islet function.

Discussion

Injection of NOD mice with antibodies directed against CSF-1R depleted the islet resident macrophages while having a variable effect on macrophages of secondary lymphoid tissues and various other organs. The treatment had a profound effect in the development of diabetes. The manner in which the islet macrophage was eliminated by the antibody treatment is not clear, although it does not involve an acute inflammatory reaction (14). The islet transcriptome analysis displayed no up-regulation of inflammatory transcripts following macrophage depletion (Fig. 2*C*). CSF-1R signaling is crucial for sustaining macrophage viability, which is most likely the reason for its loss following the antibody treatment (11).

There are two distinct scenarios that likely contributed to the attenuation of the active autoimmune process: (*i*) the impairment of islet antigen presenting function and (*ii*) the development of a regulatory process. Concerning the islets, these studies confirm the centrality of the resident macrophage in the pathophysiology of pancreatic islets. The islet macrophage arises during embryonal development. It is required for the early development of islets and during postnatal growth as is evident in the op/op mouse that lack CSF-1 (4, 5). However, in adult mice, islet function is not impaired when the macrophage is absent (our studies in B6 mice). We have not probed other possible roles for the islet macrophage such as maintaining vessel permeability, protecting against infectious agents, or modulating the physiology of beta cells. The islet macrophage is highly activated, as evidenced by their expression of TNF and IL-1 transcript and protein, and high expression levels of MHC-II (5, 10). In the context of autoimmunity, such as in NOD mice, autoreactive T cells escape thymic control and enter islets whereupon they establish long-lived contact with the macrophage (26).

The macrophage-depleted islet per se was impaired in its capacity to receive diabetogenic T cells. In their absence, lymphocyte entry into islets was impaired. The immunofluorescence and two-photon imaging of isolated islets showed the majority of CD4 T cells in islets in contact with the macrophage. Indeed, previous analyses showed macrophage filipodia extending into the blood vessel lumens (8). I.v. injecting 0.5-μm latex beads coated with antibodies to I-A^{g7} localized the beads to the macrophage/blood vessel interface. These findings point to the macrophage filopodia as the anatomical element that captures

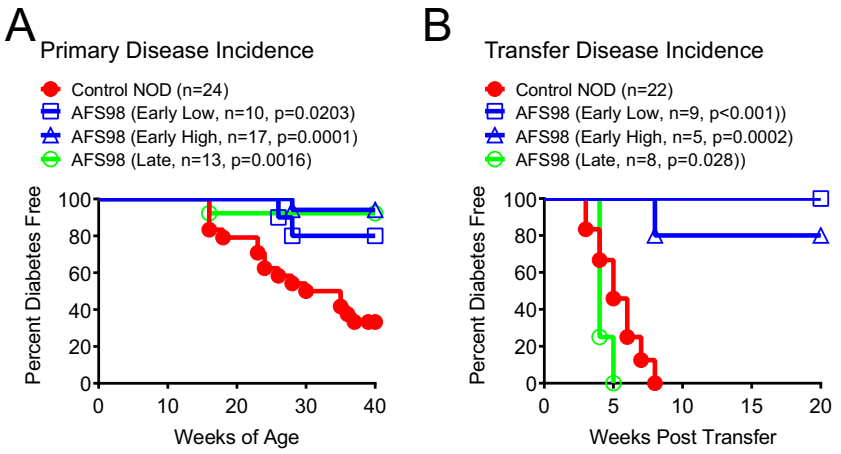

C

Protocol (Weeks/Dose of Treatment)	Primary Diabetes Incidence		Transfer Diabetes Incidence		Anti PD-1
	Control	AFS98	Control	AFS98	after AFS98 Primary
Early(3-4-5 wks/0.5-2-2 mg)	8/10 (80%)	2/10 (20%)	9/9 (100%)	0/9 (0%)	N.D.
Early(2-3-6-8-10-12 wks/0.5-2-2-2-2-2 mg)	8/14 (57%)	1/17 (6%)	5/5 (100%)	1/5 (20%)	3/3 (100%)
Late(10-12-14-16 wks/2-2-2-2 mg)	8/15 (53%)	1/13 (8%)	8/8 (100%)	8/8 (100%)	4/4 (100%)

Fig. 6. Treatment with AFS98 protects against autoimmune diabetes. (*A*) Female NOD mice were left untreated, or injected with Rat IgG2$_a$ or AFS98 at the ages and doses indicated in *C* and followed for diabetes incidence. Control mice represent the pooled results of the three experiments. (*B*) Splenocytes were isolated from nondiabetic 44- to 50-wk-old mice taken from *A*, 10^7 were transferred into NOD.*Rag1*$^{-/-}$ mice, and recipients were followed for diabetes incidence. (*C*) Summary of primary and transfer diabetes incidence for three AFS98 treatment protocols as well as the effect of PD-1 treatment on the AFS98 protection. Weeks indicate ages of mice at treatment, and dose is milligrams per mouse for either control or AFS98 antibodies.

the diabetogenic CD4 T cells, while the high-expression MHC-II may well be the key molecular substrate (8). In sum, the present and past studies point to the macrophages as the beacon, the true gatekeeper for entrance of lymphocytes into the islet.

Three pointed findings followed the initial depletion of macrophages. First, the effect of AFS98 treatment applied to mice already undergoing an active diabetogenic process. At 10 wk of age, the autoimmune process is progressing; our own studies showed a striking inflammatory signal at this time. However, AFS98 treatment at this time was effective. This indicates that AFS98 inhibits when there are active diabetogenic T cells. Thus, the inhibitory effect of macrophage depletion is not necessarily accounted for by a lack of T cell priming. Second is that after the period of macrophage depletion, the islet becomes progressively receptive to the entrance of T cells and new macrophages. This was evident when examining the islets by flow cytometry. Despite this renewed accumulation of leukocytes into the islets, the beta cells were preserved. Histological examination at the 42-wk period showed the preservation of beta cells, albeit many islets showed the peri-insulitic lesion next to otherwise normal beta cells. This finding suggests that the newly arriving monocyte-derived macrophages or other cells in islets or in lymph nodes are not driving forward the process and may participate by controlling it. For example, the incoming macrophages may be inhibitory in a way akin of what happens in the tumor environment. Finally, a regulatory process involving the PD-1 and PD-L1 interacting molecules was evident. The mice protected by AFS98 until over 40 wk of age developed diabetes if given anti–PD-1. At face value, this result tells us that the active process had been under checkpoint control following the initial macrophage deletion.

Future studies should examine the site of the control pathway, whether it is the lymph nodes or the islets, many of which had the peri-insulitic lesion. In NOD diabetogenicity, peripheral lymph nodes play a key role in the early program of the autoimmunity (27–29). We did show here that the lymph nodes after AFS treatment could be an effective site of presentation of either diabetogenic or foreign antigens. It is not because of the lack of presenting function in lymph nodes that diabetes is curtailed. However, the nodes could be the anatomical substrate of the regulatory process involving the PD-1/PD-L1 pathway. The lymph nodes are depleted of their resident macrophages, albeit not to the extent as islets. Thus, the presentation that results in the activation of the PD-1/PD-L1 activation could be caused by DC or B cells. Lymph node macrophages at face value would foster positive interactions in a normal situation but, in their absence, would drive the process into a regulatory pathway. In our early studies, we did find that the F4/80 positive macrophages were capable of presenting minor epitopes of insulin.

Various inflammatory processes have been studied with variable results using antibodies to transiently remove tissue macrophages (30–35). Other treatment modalities have targeted blood monocytes. Clodronate-liposome treatment depletes circulating monocytes and affected a number of inflammatory reactions (36). These treatments over repeated periods of time resulted in the reduction in diabetes in NOD mice (36–40). In all of these instances, the reduction resulted in the loss of inflammatory macrophages, i.e., macrophages derived from monocytes that participated as effectors in the diabetogenic process. A study by Calderon et al. (41) showed that resident macrophages were not affected by injections of clodronate liposomes, although diabetes induced by the transfer of the activated BDC2.5 CD4$^+$ T cells was affected. Diabetes induced by such transfer required the presence of new macrophages as effector cells modulated by IFN-γ production from activated T cells (42).

Integrating our findings with these, it is evident that macrophages have two distinct functions in autoimmune diabetes: First, as evident here, as a cell controlling the development and progression of the diabetogenic process, and second, as an effector cell once islet inflammation is induced.

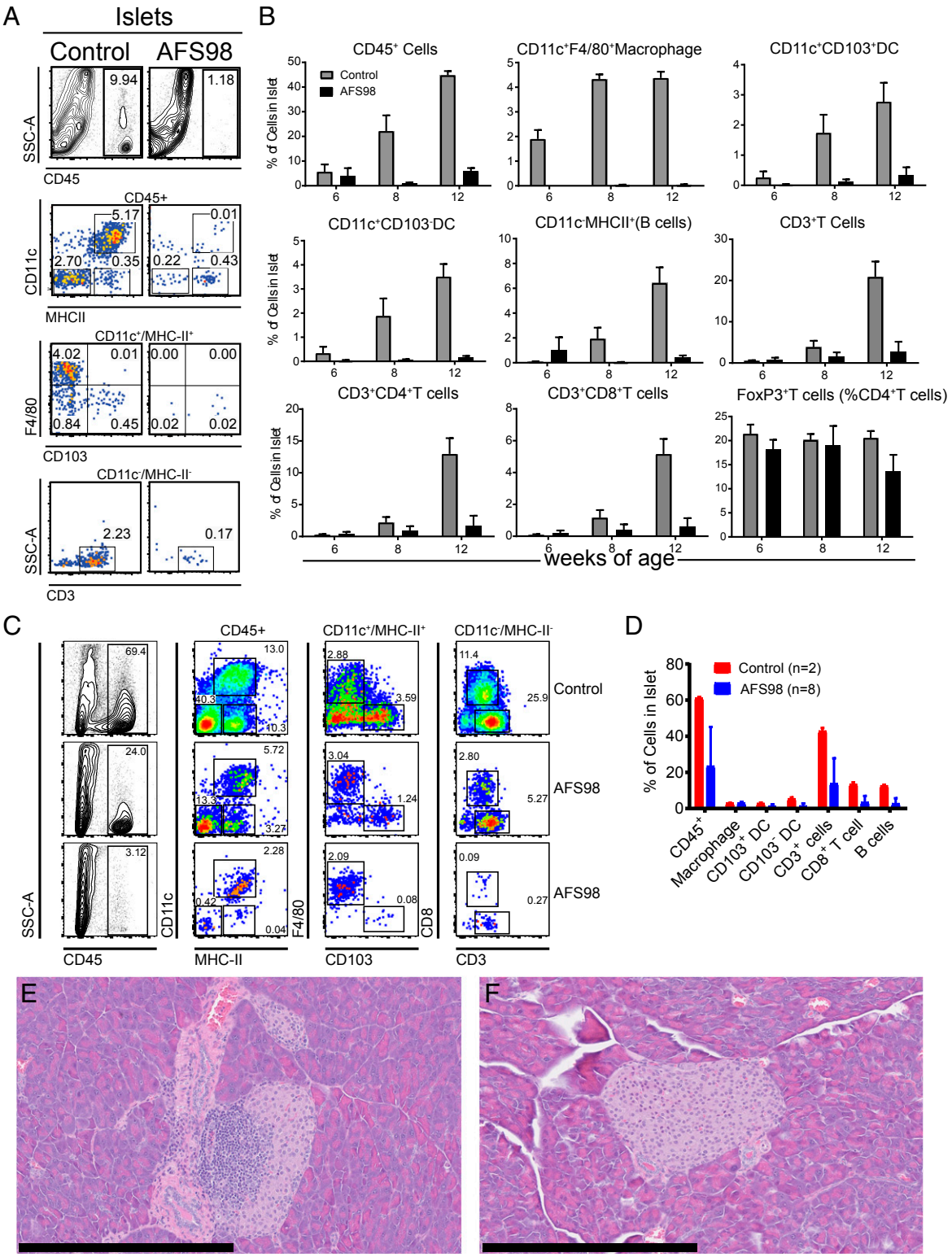

Fig. 7. Early treatment with AFS98 reduces infiltrating leukocytes in NOD mice up to 12 wk of age. (*A* and *B*) Female NOD mice were left untreated or injected with 0.5 mg of AFS98 i.p. at 2 wk of age and 2.0 mg of AFS98 i.p. at 4, 7, and 10 wk of age. The islets of mice at 6 (*B*), 8 (*A* and *B*), and 12 (*A*) wk of age were isolated and analyzed by flow cytometry. (*A*) Shows the flow cytometry plots of myeloid and T cell compartments. Gating is indicated over the plots. Flow cytometry plots are representative of individual islet preparation from three control or four AFS98-treated mice. (*B*) Summarizes the flow cytometry data for all time course experiments (three to four mice per group). Bars represent the mean ± SD for two independent experiments with two to three replicates per group. (*C*) Flow cytometry plots of immune cell populations in islets isolated from nondiabetic control or AFS98-treated mice taken from Fig. 6 *A* and *C* early treatment examined at 40–44 wk of age. Plots were generated from individual mice. Gates are indicated on the *Top* of each column of plots. Flow cytometry plots are representative of individual islets preparations isolated from two control and eight AFS98-treated mice. (*D*) Summary of the data shown in *C*. (*E* and *F*) Hematoxylin/eosin staining of pancreatic sections isolated from nondiabetic AFS98-treated mice taken from Fig. 6*A*: The mice were treated early, and their islets were examined at 40–44 wk of age. (Scale bars, 400 μm.)

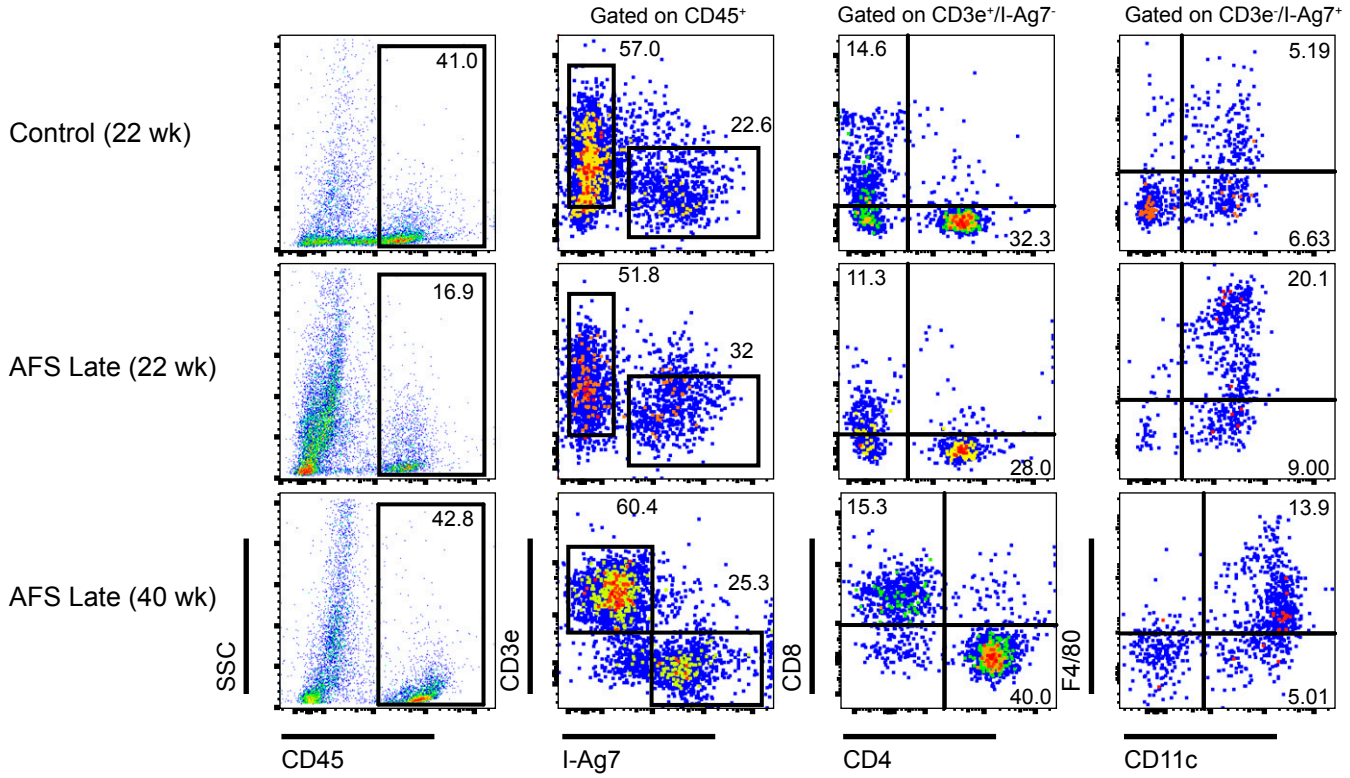

Fig. 8. Leukocyte infiltrates are reduced following macrophage depletion at 10 wk of age. NOD mice were either treated with AFS98 or control Rat IgG2$_a$ starting at 10 wk of age. At 22 or 40 wk of age, the islet cells of control or AFS-treated mice were isolated and analyzed by flow cytometry as indicated. Values in the CD45 by SSC plot represent the percent of leukocytes in islets. Values in the CD3e by I-A^{g7} plot represent the percent CD3e$^+$ or I-A^{g7+} cells as a percent of CD45$^+$ cells. Values in the T cell (CD3e$^+$, I-A^{g7-}) and APC (CD3e$^-$, I-A^{g7+}) plots represent the percent of cells in each quadrant as a function of total islet cellularity. Gating is indicated over the top for each column of plots. Results are representative of two mice per group.

Materials and Methods

Mice. Female C57BL/6 mice (B6), female NOD/ShiLtJ (NOD), NOD.129S7(B6)-*Rag1*^{tm1Mom}/J (NOD.*Rag1*$^{-/-}$), NOD.Cg-Tg(TcraBDC2.5,TcrbBDC2.5)1Doi/DoiJ (BDC2.5), and NOD.Cg-Tg(TcraTcrbNY8.3)1Pesa/DvsJ (NY8.3) mice were purchased from the Jackson Laboratories and bred in house. NY8.3 mice were backcrossed onto the congenic NOD.B6-*Ptprc*^{b}/6908MrkTacJ (NOD.CD45.2) background for T cell transfer experiments (18). All mouse experiments were performed in accordance with the Division of Comparative Medicine of Washington University School of Medicine [Association for Assessment and Accreditation of Laboratory Animal Care (AAALAC) accreditation no. A3381-01].

T Cell Transfer Assay; ELISPOT; Anti–PD-1 Treatment. 8F10, BDC2.5, and NY8.3 TCR transgenic mouse spleens and lymph nodes were harvested and dispersed into single-cell suspensions. CD4- or CD8-positive cells were selected via magnetic microbead cell separation (Miltenyi Biotech) according to the manufacturer's protocol. The cells were then stained with 1 μM carboxyfluorescein diacetate succinimidyl ester (Life Technologies) for 15 min at 37 °C and immediately quenched with 4 °C DMEM supplemented with 10% FCS. CFSE-labeled cells (3.0×10^6) were then transferred into recipient mice via tail vein injections. Islets, draining pancreatic lymph nodes, and inguinal lymph nodes were harvested, dispersed into single-cell populations, and stained with fluorescent antibodies for analyses by flow cytometry. For experiments dealing with anti–PD-1, AFS98-treated or control NOD mice were injected with 200 μg of antibody three times over 6 d (days 0, 3, and 6; Anti–PD-1 clone RMP1-4; Leinco Technologies). Mice were then followed for diabetes incidence. For experiments examining the lymph node response by ELSIPOT, B6.g7 or NOD mice (7–10 wk old) were treated with a single 2.0-mg dose of AFS98 or control rat IgG2a. Seven days later, the mice were immunized in the footpad with 10 nmol INS B:9–23 peptide, HEL protein (Sigma-Aldrich), or IGRP:206–214 peptide. After 7 d, the animals were killed and the popliteal lymph nodes were removed and made into single-cell suspensions. Lymph nodes were assayed for reactivity by eliciting a recall response on either IL-2 or IFN-γ–coated 96-well multiscreen plates (MilliporeSigma) for ELISPOT. One million popliteal lymph node cells were plated per well with 10 μM antigen, and reactive cells were counted using Immunospot Software (C.T.L.). Immune responses in mice challenged with INS B:9–23 peptide were recalled with either insulin or INS B:9–23. Immune responses in mice challenged with HEL protein were recalled with either HEL protein or HEL peptides 11–25 (CD4 epitope) or 20–35 (CD8 epitope). Finally, responses in mice challenged with IGRP:206–214 peptide were recalled with either IGRP:128–142 (CD4 epitope) or IGRP:206–214 (CD8 epitope).

Glucose Tolerance Assay and Insulin Quantitation. For glucose tolerance experiments, female B6 mice were maintained on a normal diet and then fasted overnight for 12 h. Fasting blood glucose levels were tested before a challenge with 1.5 g/kg glucose in PBS (Life Technologies) administered by i.p. injection. Blood glucose was measured at the intervals indicated in the experiments. For insulin quantitation, control or αCSF-1R–treated mice were maintained on 20% sucrose water for 7 d, returned to regular water for an additional 2 d, fasted overnight, and then their pancreata were removed and weighed. Pancreata was minced and homogenized. The supernatant was collected after pelleting the homogenate, and insulin was quantified using the Rat Insulin Radioimmune Assay (MilliporeSigma), as per the manufacturer's instruction.

Antigen Presentation Assay. Islets were dispersed nonenzymatically, and 4.0×10^4 islet cells per well were plated together in a 96-well plate with 5.0×10^4 T cell hybridoma cells per well, in DMEM containing 10% FCS and 5 mM or 25 mM glucose (low or high glucose media, respectively). After 24 h, the supernatants were removed and the production of IL-2 was measured by culturing supernatants in the presence of the IL-2–dependent cell line, CTLL-2. Proliferation of CTLL-2 cells was measured by the incorporation of ^{3}[H] thymidine. For the antigen presentation assays, the 8F10 and IIT3 T cell hybridomas directed to the insulin B:12–20, and B:13–21 epitopes, respectively, were used (7).

Histology and Imaging. Microscopy imaging was performed using an Eclipse E800 microscope (Nikon) equipped with CFI Plan Apo Lambda DM 20× air objective, X-Cite 120PC light source (Excelitas Technologies), EXi blue fluorescence microscopy camera, and QCapture 64-bit v2.9.13 acquisition software (QImaging).

Islets, Pancreatic Stroma, and Lymph Node Isolation. Pancreata were perfused through the common bile duct with 5.0 mL of calcium-free HBSS supplemented with 400.0 μg/mL of collagenase. Pancreata were then removed, and digested in a 37 °C water bath followed by vigorous shaking for 90 s, washed three times in HBSS, and then passed through a 70.0-μm strainer to retain the islets. Cells that passed the through the strainer represented the pancreatic stroma and were filtered a second time through a 40.0-μm filter to prepare a single-cell suspension. Islets retained on the 70.0-μm filter were then flushed into a Petri dish for hand-picking using a zinc-chelating dye, Dithizone (200 μg/mL 10% DMSO PBS; Sigma), to identify the islets. Hand-picked islets were then dispersed using Cell Dissociation Solution Non-Enzymatic (Sigma) for 10 min at 37 °C. Lymph nodes and spleens were digested by incubation at 37 °C in DMEM supplemented with 10% fetal calf-serum, 125 μg/mL Liberase TL (Roche Life Science), and 50 μg/mL DNase I (Roche Life Science). All single-cell suspensions were then incubated with 2.4G2 conditioned media (PBS, 1% BSA, and 50% 2.4G2 in DMEM) at 4 °C for 15 min to block FC receptors. Samples were then stained with fluorescent antibodies for flow cytometry or sorting.

Antibodies for Flow Cytometry and Sorting. Flow cytometry data were acquired on a FACSCanto II (BD Biosciences) and analyzed on FlowJo v10.2 software (FlowJo, LLC). Cell sorting was performed using a FACSAria II (BD Biosciences). The following antibodies were purchased from BioLegend: BV510 anti-CD45 (30-F11), Pacific Blue (PB) anti–I-A/I-E (pan MHC-II), FITC anti-CD3 (2C11), FITC and APC anti-F4/80 (BM8), PE-Cy7 anti-CD11b (M1/70), PE anti-CD103 (2E7), PerCP-Cy5.5 anti-Ly6C (AL-21), PerCP-Cy5.5 anti-B220 (RA3-6B2), and APC anti-CD64 (X54-5/7/1). APC-eFluor780 anti-CD11c (N418), PerCP-eFluor710 anti-CD8 (53-6.7), eFluor450 anti–Ki-67 (SolA15), and APC FoxP3 (FJK-16) were purchased from eBioscience. For intracellular staining, the FoxP3 Fix/Perm kit (eBioscience) was used according to the manufacturer's instructions.

ACKNOWLEDGMENTS. We thank Pavel Zakharov who helped us in discussions and in experiments. Katherine Fredericks was responsible for our NOD mouse colony, Nick Benschoff helped with islet isolation, and Brian Saunders helped with the microscopy experiments. We are supported by a Janssen-Washington University cooperative agreement and by National Institute of Health Grants AI114551 and K058177. The laboratory receives general support from the Kilo Diabetes and Vascular Research Foundation.

1. Perdiguero EG, Geissmann F (2016) The development and maintenance of resident macrophages. *Nat Immunol* 17:2–8.
2. Mass E, et al. (2016) Specification of tissue-resident macrophages during organogenesis. *Science* 353:aaf4238.
3. Wiktor-Jedrzejczak W, et al. (1990) Total absence of colony-stimulating factor 1 in the macrophage-deficient osteopetrotic (op/op) mouse. *Proc Natl Acad Sci USA* 87: 4828–4832.
4. Banaei-Bouchareb L, et al. (2004) Insulin cell mass is altered in Csf1op/Csf1op macrophage-deficient mice. *J Leukoc Biol* 76:359–367.
5. Calderon B, et al. (2015) The pancreas anatomy conditions the origin and properties of resident macrophages. *J Exp Med* 212:1497–1512.
6. Ferris ST, et al. (2017) The islet-resident macrophage is in an inflammatory state and senses microbial products in blood. *J Exp Med* 214:2369–2385.
7. Vomund AN, et al. (2015) Beta cells transfer vesicles containing insulin to phagocytes for presentation to T cells. *Proc Natl Acad Sci USA* 112:E5496–E5502.
8. Calderon B, Carrero JA, Miller MJ, Unanue ER (2011) Cellular and molecular events in the localization of diabetogenic T cells to islets of Langerhans. *Proc Natl Acad Sci USA* 108:1561–1566.
9. Carrero JA, Calderon B, Towfic F, Artyomov MN, Unanue ER (2013) Defining the transcriptional and cellular landscape of type 1 diabetes in the NOD mouse. *PLoS One* 8:e59701.
10. Ferris ST, et al. (2014) A minor subset of Batf3-dependent antigen-presenting cells in islets of Langerhans is essential for the development of autoimmune diabetes. *Immunity* 41:657–669.
11. Sudo T, et al. (1995) Functional hierarchy of c-kit and c-fms in intramarrow production of CFU-M. *Oncogene* 11:2469–2476.
12. MacDonald KPA, et al. (2010) An antibody against the colony-stimulating factor 1 receptor depletes the resident subset of monocytes and tissue- and tumor-associated macrophages but does not inhibit inflammation. *Blood* 116:3955–3963.
13. Sauter KA, et al. (2014) Pleiotropic effects of extended blockade of CSF1R signaling in adult mice. *J Leukoc Biol* 96:265–274.
14. Hume DA, MacDonald KPA (2012) Therapeutic applications of macrophage colony-stimulating factor-1 (CSF-1) and antagonists of CSF-1 receptor (CSF-1R) signaling. *Blood* 119:1810–1820.
15. Kopf M, Schneider C, Nobs SP (2015) The development and function of lung-resident macrophages and dendritic cells. *Nat Immunol* 16:36–44.
16. Sierro F, et al. (2017) A liver capsular network of monocyte-derived macrophages restricts hepatic dissemination of intraperitoneal bacteria by neutrophil recruitment. *Immunity* 47:374–388.e6.
17. Mohan JF, et al. (2010) Unique autoreactive T cells recognize insulin peptides generated within the islets of Langerhans in autoimmune diabetes. *Nat Immunol* 11: 350–354.
18. Delong T, et al. (2012) Diabetogenic T-cell clones recognize an altered peptide of chromogranin A. *Diabetes* 61:3239–3246.
19. Lieberman SM, et al. (2003) Identification of the beta cell antigen targeted by a prevalent population of pathogenic CD8+ T cells in autoimmune diabetes. *Proc Natl Acad Sci USA* 100:8384–8388.
20. Wang J, et al. (2010) In situ recognition of autoantigen as an essential gatekeeper in autoimmune CD8+ T cell inflammation. *Proc Natl Acad Sci USA* 107:9317–9322.
21. Ansari MJI, et al. (2003) The programmed death-1 (PD-1) pathway regulates autoimmune diabetes in nonobese diabetic (NOD) mice. *J Exp Med* 198:63–69.
22. Fife BT, et al. (2006) Insulin-induced remission in new-onset NOD mice is maintained by the PD-1-PD-L1 pathway. *J Exp Med* 203:2737–2747.
23. Wang J, et al. (2005) Establishment of NOD-Pdcd1-/- mice as an efficient animal model of type I diabetes. *Proc Natl Acad Sci USA* 102:11823–11828.
24. Keir ME, et al. (2006) Tissue expression of PD-L1 mediates peripheral T cell tolerance. *J Exp Med* 203:883–895.
25. Eppihimer MJ, et al. (2002) Expression and regulation of the PD-L1 immunoinhibitory molecule on microvascular endothelial cells. *Microcirculation* 9:133–145.
26. Mohan JF, et al. (2017) Imaging the emergence and natural progression of spontaneous autoimmune diabetes. *Proc Natl Acad Sci USA* 114:E7776–E7785.
27. Levisetti MG, Suri A, Frederick K, Unanue ER (2004) Absence of lymph nodes in NOD mice treated with lymphotoxin-beta receptor immunoglobulin protects from diabetes. *Diabetes* 53:3115–3119.
28. Gagnerault M-C, Luan JJ, Lotton C, Lepault F (2002) Pancreatic lymph nodes are required for priming of beta cell reactive T cells in NOD mice. *J Exp Med* 196:369–377.
29. Wan X, Thomas JW, Unanue ER (2016) Class-switched anti-insulin antibodies originate from unconventional antigen presentation in multiple lymphoid sites. *J Exp Med* 213: 967–978.
30. Murayama T, et al. (1999) Intraperitoneal administration of anti-c-fms monoclonal antibody prevents initial events of atherogenesis but does not reduce the size of advanced lesions in apolipoprotein E-deficient mice. *Circulation* 99:1740–1746.
31. Segawa M, et al. (2008) Suppression of macrophage functions impairs skeletal muscle regeneration with severe fibrosis. *Exp Cell Res* 314:3232–3244.
32. Lim AKH, et al. (2009) Antibody blockade of c-fms suppresses the progression of inflammation and injury in early diabetic nephropathy in obese db/db mice. *Diabetologia* 52:1669–1679.
33. Kubota Y, et al. (2009) M-CSF inhibition selectively targets pathological angiogenesis and lymphangiogenesis. *J Exp Med* 206:1089–1102.
34. Huynh D, et al. (2009) Colony stimulating factor-1 dependence of paneth cell development in the mouse small intestine. *Gastroenterology* 137:136–144e3.
35. Hashimoto D, et al. (2011) Pretransplant CSF-1 therapy expands recipient macrophages and ameliorates GVHD after allogeneic hematopoietic cell transplantation. *J Exp Med* 208:1069–1082.
36. Van Rooijen N, Sanders A (1994) Liposome mediated depletion of macrophages: Mechanism of action, preparation of liposomes and applications. *J Immunol Methods* 174:83–93.
37. Lee KU, Amano K, Yoon JW (1988) Evidence for initial involvement of macrophage in development of insulitis in NOD mice. *Diabetes* 37:989–991.
38. Ihm SH, Lee KU, Yoon JW (1991) Studies on autoimmunity for initiation of beta-cell destruction. VII. Evidence for antigenic changes on beta-cells leading to autoimmune destruction of beta-cells in BB rats. *Diabetes* 40:269–274.
39. Jun HS, Santamaria P, Lim HW, Zhang ML, Yoon JW (1999) Absolute requirement of macrophages for the development and activation of beta-cell cytotoxic CD8+ T-cells in T-cell receptor transgenic NOD mice. *Diabetes* 48:34–42.
40. Jun HS, Yoon CS, Zbytnuik L, van Rooijen N, Yoon JW (1999) The role of macrophages in T cell-mediated autoimmune diabetes in nonobese diabetic mice. *J Exp Med* 189: 347–358.
41. Calderon B, Suri A, Unanue ER (2006) In CD4+ T-cell-induced diabetes, macrophages are the final effector cells that mediate islet β-cell killing: Studies from an acute model. *Am J Pathol* 169:2137–2147.
42. Calderon B, Suri A, Pan XO, Mills JC, Unanue ER (2008) IFN-gamma-dependent regulatory circuits in immune inflammation highlighted in diabetes. *J Immunol* 181: 6964–6974.

Supporting Information

Carrero et al. 10.1073/pnas.1713543114

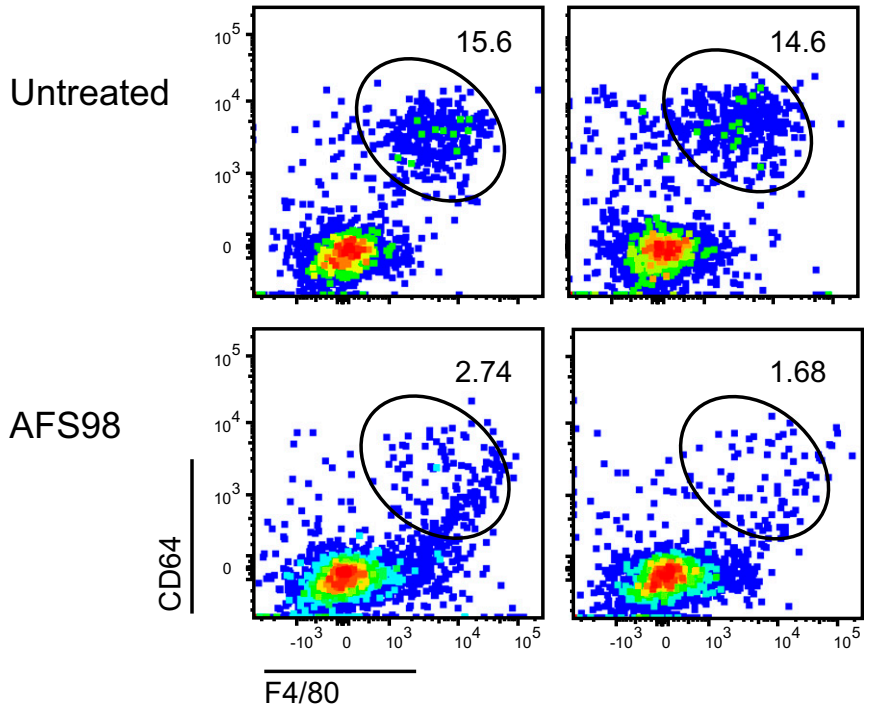

Fig. S1. Pancreatic stromal macrophages are reduced following AFS98 treatment. B6 mice were treated as in Fig. 1 and analyzed for the presence of $CD45^+F4/80^+CD64^+$ macrophages. Numbers indicate the percentage of macrophages in the pancreatic stroma as a percent of the $CD45^+$ cells. Cells were gated on FSC/SSC/$CD45^+$. Data are taken from two independent mice per group and is representative of two independent experiments.

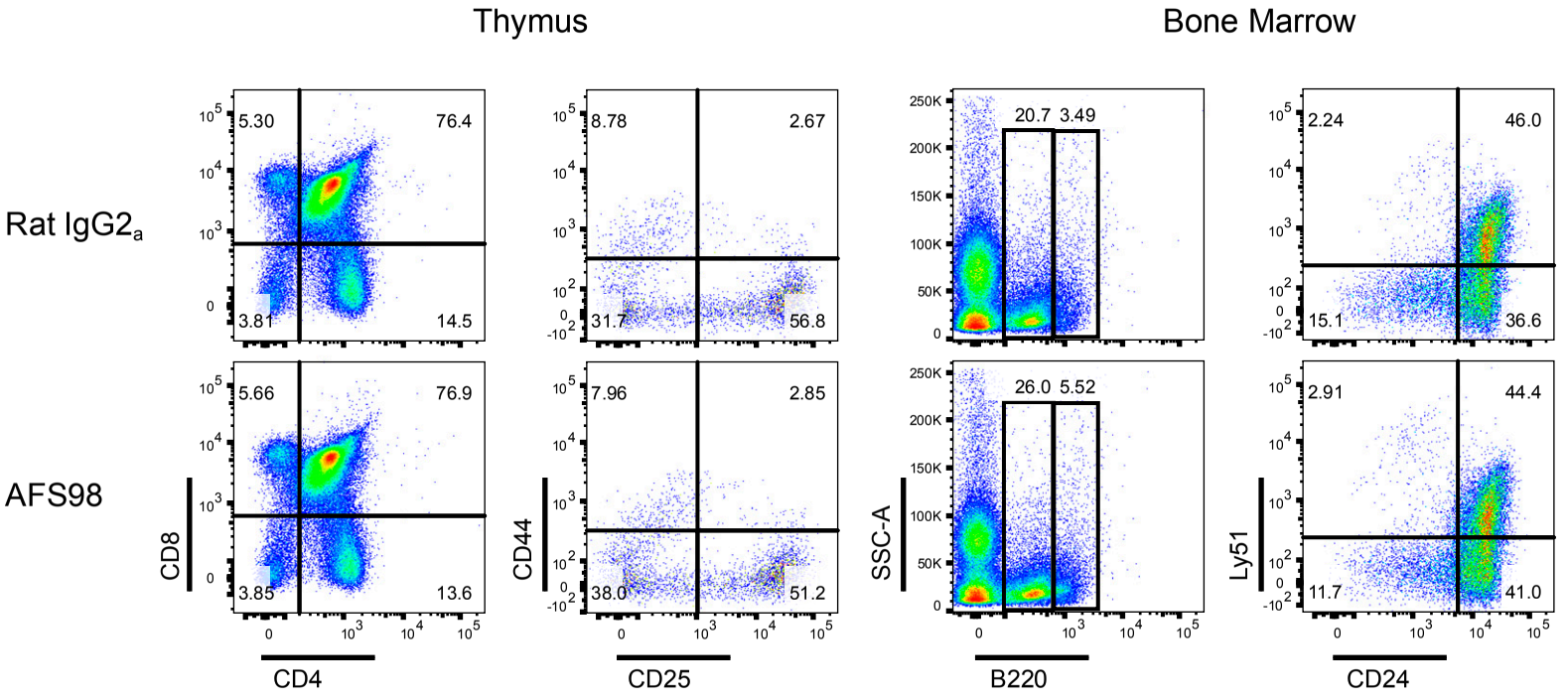

Fig. S2. Thymic T cells and bone marrow B cells are grossly normal following AFS98 treatment. Male NOD mice were injected with 2 mg of either AFS98 or Rat $IgG2_a$ at 4 wk of age and then sampled at 6 wk of age. Thymus and bone marrow were harvested, and single-cell suspensions were generated. Cells were evaluated by flow cytometry. For thymus, cells were first gated on forward and side scatter, and $CD45^+$ then CD4 by CD8 was plotted. Next, the CD4/CD8 double negative population was gated and examined for CD44 and CD25 as plotted on the *Right*. For bone marrow, cells were gated by forward and side scatter, and then plotted for B220 expression. The B220 intermediate cells were then gated and plotted for CD24 and Ly51 staining as shown on the *Right*. Numbers indicate the percentage of cells in each region as a function of the total cells in the plot. Results are representative of three individual mice per group.

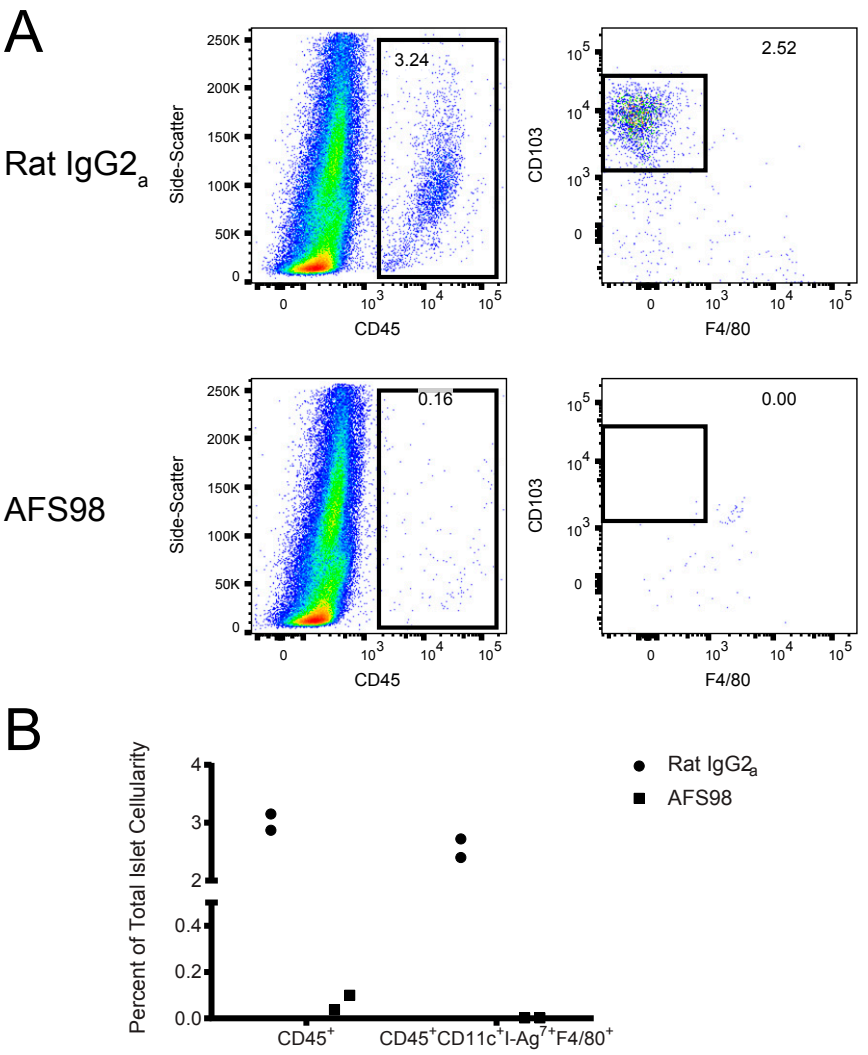

Fig. S3. AFS98 depletes islet macrophages in the NOD.*Rag1*$^{-/-}$ mouse. Female NOD.*Rag1*$^{-/-}$ mice were treated at 4 wk of age with 2 mg of either rat IgG2$_a$ or ASF98 and then sampled at 6 wk of age. (*A* and *B*) Islet leukocytes cells were analyzed by flow cytometry. Cells were gated by forward and side scatter and then plotted for CD45 (*Left*). Next, cells were gated on CD45$^+$CD11c$^+$I-Ag7$^+$, and the F4/80 by CD103 cells were plotted (*Right*). Values represent the percent of each box as a function of total islet cellularity. (*B*) Scatter plots of the percent of CD45$^+$ or F4/80$^+$CD45$^+$CD11c$^+$I-Ag7$^+$ in two individual mice per group.

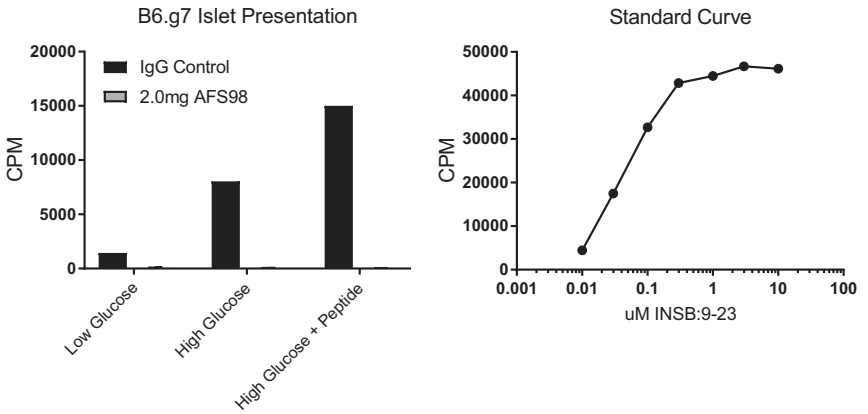

Fig. S4. Depletion of macrophages blocks MHC-II antigen presentation by whole islet cells. Antigen presentation was performed as in Fig. 3*B* except with 6-wk-old B6.g7 mice that were given 2 mg of either control or AFS98 antibody at 4 wk of age. *Left* shows the CTLL-2 assay for an anti-insulin CD4 T cell hybridoma. *Right* shows the peptide curve of the hybridoma using an immortalized cell line as APC.